

Nonlocal couplings, off-shell effects, and the nuclear response

F. A. Brieva^(1,2) and W. G. Love⁽¹⁾

⁽¹⁾*Department of Physics and Astronomy, University of Georgia, Athens, Georgia 30602*

⁽²⁾*Departamento de Física, Facultad de Ciencias Físicas y Matemáticas, Universidad de Chile Casilla 487-3, Santiago, Chile*

(Received 18 December 1989)

We study momentum-dependent or nonlocal couplings and off-shell effects in the internucleon force arising from antisymmetrization for inclusive nucleon scattering over a wide range of momentum transfer and energy loss to the target. Our results illustrate that spin observables are more sensitive to these couplings than are unpolarized cross sections. The experimental results can be understood in terms of the nuclear response function with an uncertainty of $\sim 10\%$ for incident nucleons above 300 MeV. At incident energies near ~ 100 MeV and below, the nonlocal couplings are much more important and cannot reliably be neglected. The sensitivity of inclusive nucleon scattering to the choice of effective nucleon-nucleon interaction is also found to be generally non-negligible.

I. INTRODUCTION

The study of nucleon inelastic scattering to the continuum is a rich and widely used approach for learning about those modes of nuclear excitation involving large momentum transfer and energy loss to the target nucleus. Under these conditions we expect to learn primarily about the nuclear response function and the underlying interaction which mediates the reaction. However, when nucleons are used as probes, we face the problem of accounting for the indistinguishability of the interacting particles as well as for the off-shell properties of the effective internucleon force. This situation is quite different from that encountered in processes induced by electrons where, due to the well-understood and relatively simple electromagnetic coupling, electron-scattering data yield a direct measurement of the nuclear response function.¹

The most common theoretical approach to the calculation of the inclusive cross section for inelastic nucleon scattering has been based on the assumption that the nucleon-nucleon cross section in the medium can be factorized from the nuclear response.^{2,3} This idea, originally proposed for high-energy nucleons (above 500 MeV), relatively small momentum transfer ($q \lesssim 0.5 \text{ fm}^{-1}$), and energy loss to the target ($\omega \lesssim 30 \text{ MeV}$), has been extended nonrelativistically⁴ and relativistically⁵ to analyze a diversity of experimental data obtained under conditions well outside the ranges where the theory was developed. A similar approach has been recently applied to understand contributions from single-particle excitations in the pre-equilibrium region⁶ at energies below 100 MeV. Although attractive by its simplicity, the assumed factorized structure of the inclusive nucleon cross section deserves a more quantitative evaluation. The extent to which the motion of the target nucleons may be neglected or approximated depends on the projectile energy, the momentum transfer, and the range of excitation energy. In general, the nucleon-nucleon amplitude needs to be evaluated off shell in the nuclear medium. Furthermore, the relative importance of the different components of the

internucleon force changes as the momentum transfer increases,⁷ making some observables more sensitive to the factorization of the response function and the nucleon-nucleon cross section. An indication of the importance of these effects can be found in the calculation of the optical potential at intermediate energies^{8,9} (200–400 MeV) where the factorized $t\rho$ model fails to reproduce the elastic-scattering data. By contrast, approaches^{8,9} which account explicitly for the off-shell properties of the internucleon force provide significantly better descriptions of the data.

In this paper we evaluate the inclusive nucleon cross section and spin-transfer observables within the context of an interacting Fermi-gas model to first order in the projectile-nucleon effective interaction. Particular attention is paid to the role of the effective internucleon force and the associated effects due to antisymmetrization. Since we are mainly interested in the region of momentum transfer to the target greater than 1.0 fm^{-1} and rather large excitation energies, we have considered the polarization propagator to first order, including consistently the widths for particle states.¹⁰ The effects of distortion in entrance and exit channels are treated in an eikonal approximation.^{3,4} In order to account for finite-size effects of the target nucleus, results for infinite nuclear matter are applied within a local-density approximation. Thus we obtain a parameter-free model for describing the inelastic process. By including the nonlocal couplings associated with antisymmetrization between the projectile and target nucleons explicitly, we obtain an estimate of the range of validity of the “standard” model,^{3–6} which assumes a direct relation between the inclusive cross section and the nuclear response function. Alternatively, our calculations will show how inelastic nucleon scattering samples information beyond the usual nuclear response and, indeed, yields information on the polarization propagator in the medium. In addition to estimating the range of validity of the standard model, we also illustrate the level of uncertainty associated with the choice of effective nucleon-nucleon interaction used for calculating the inclusive observables.

II. INCLUSIVE NUCLEON SCATTERING

For simplicity, we develop the present approach to the calculation of the inclusive nucleon cross section in a nonrelativistic framework. Relativistic kinematics are included in the results presented in Sec. III. We consider an incident nucleon with momentum \mathbf{k} , kinetic energy E , and spin-isospin quantum numbers represented by i ; in the final state we assume that a nucleon with momentum \mathbf{k}' and spin-isospin quantum numbers f is measured. Assuming a one-step process as the relevant reaction mechanism, the inclusive cross section per unit of solid angle Ω and energy loss to the target ω is given by

$$\frac{d^2\sigma}{d\Omega d\omega} = K \left(\frac{k'}{k} \right) \sum_n \delta[\omega - (E_n - E_0)] |T_{n0}(\mathbf{k}', f; \mathbf{k}, i)|^2, \quad (1)$$

where E_0 (E_n) are the target ground- (excited-) state en-

$$\frac{d^2\sigma}{d\Omega d\omega} = K \left(\frac{k'}{k} \right) \sum_{\alpha, \beta, \gamma, \delta \leq \epsilon_F} \langle \varphi_{\mathbf{k}, i}^{(+)} \phi_\gamma | T^+(E + \epsilon_\gamma) | \varphi_{\mathbf{k}, f}^{(-)} \phi_\delta \rangle_A S(\omega) \langle \varphi_{\mathbf{k}', f}^{(-)} \phi_\beta | T(E + \epsilon_\alpha) | \varphi_{\mathbf{k}, i}^{(+)} \phi_\alpha \rangle_A, \quad (3)$$

with $\langle T \rangle_A$ the antisymmetrized matrix elements of the internucleon effective force T in the medium obtained from the nucleon-nucleon force evaluated at the total energy of the interacting pair, $\{\varphi^{(\pm)}\}$ are the incident and exit distorted-wave functions with the appropriate boundary conditions, $\{\phi_\alpha\}$ are the single-particle wave functions with energy eigenvalues ϵ_ω , and ϵ_F is the target Fermi energy. $S(\omega)$ is the structure function which is defined in terms of the polarization propagator¹² Π by

$$S(\omega) = -\frac{1}{\pi} [\Pi(\omega)]. \quad (4)$$

Equation (3) is, in principle, the exact one-step contribution to the inclusive cross section. Attempts to calculate Eq. (3) in finite nuclei have been reported in Ref. 13 by simplifying the transition amplitude in order to isolate the explicit response function.

At this level we assume that distorted waves in both the entrance and exit channels, respectively, can be described in an eikonal approximation at the corresponding local momentum of the incident and outgoing particles in the medium. The imaginary distorting potentials used here were calculated from Table 4 of Ref. 14 for $E < 160$ MeV. For $E > 160$ MeV, the imaginary potential was taken to be $W = -0.6pE$ as suggested in Ref. 6. Furthermore, the ground and excited states of the target will be described by an interacting Fermi-gas model at the corresponding Fermi momentum k_F . Although the low-lying excited states are poorly described by this model, we focus on the region of momentum transfer and energy loss to the target where explicit shell effects should be unimportant. The present approximation should, therefore, provide the correct overall trend of the experimental measurements.

In this work attention is focused on the role of the transition amplitude. In a momentum representation, the two-body effective interaction may be expressed as

$$\langle \mathbf{k}' \mathbf{p}' | T(\mathcal{E}) | \mathbf{k} \mathbf{p} \rangle = \delta(\mathbf{k}' + \mathbf{p}' - \mathbf{k} - \mathbf{p}) \langle \frac{1}{2}(\mathbf{k}' - \mathbf{p}') | t(\mathcal{E} - (\mathbf{k} + \mathbf{p})^2/2M) | \frac{1}{2}(\mathbf{k} - \mathbf{p}) \rangle, \quad (5)$$

where \mathcal{E} is the total energy of the interacting pair, $t(z)$ is the one-body t matrix, and M is the total mass of the pair. Considering that the energy of a bound particle in an interacting Fermi gas is given by¹⁵

$$e(p) = \frac{p^2}{2m} + V(p), \quad (6)$$

with m the nucleon mass and $V(p)$ the real part of the self-energy in the medium, the effective force $T(\mathcal{E})$ in Eq. (3) can be approximated by

$$\langle \mathbf{k}' \mathbf{p}' | T(E + e(p)) | \mathbf{k} \mathbf{p} \rangle \simeq \delta(\mathbf{k}' + \mathbf{p}' - \mathbf{k} - \mathbf{p}) \langle \frac{1}{2}(\mathbf{k}' - \mathbf{p}') | t(E/2) | \frac{1}{2}(\mathbf{k} - \mathbf{p}) \rangle, \quad (7)$$

where E is the energy of the incident nucleon and we have neglected p and the self-energy $V(p)$ in evaluating the energy in the center of mass for the force. Equation (7) shows explicitly that the calculation of the inclusive cross section requires the off-shell properties of the nucleon-nucleon effective interaction. On-shell variants of Eq. (7) do exist.^{4,6} How-

ergies, and T_{n0} is the inelastic transition amplitude from the initial state with incident nucleon (\mathbf{k}, i, E) and target in its ground state ($n=0$) to a final state with outgoing (\mathbf{k}, f, E') and target in the excited state n . The sum over n runs over all possible excited states of the system for an energy loss $\omega = E - E'$. The constant K is

$$K = \left(\frac{2\pi}{\hbar c} \right)^4 \mathcal{E}_i \mathcal{E}_f, \quad (2a)$$

with \mathcal{E}_i (\mathcal{E}_f) the relativistic generalization of the reduced mass in the initial (final) channel. In particular,

$$\mathcal{E}_i = \frac{E_{1i} E_{2i}}{E_{1i} + E_{2i}}, \quad \mathcal{E}_f = \frac{E_{1f} E_{2f}}{E_{1f} + E_{2f}}. \quad (2b)$$

E_1 and E_2 are the total energies of the projectile and target, respectively.

Considering a single-particle description of the target, the inclusive cross section becomes¹¹

ever, calculations using the full off-shell interaction and on-shell approximations to it differ considerably in describing nucleon elastic-scattering data,^{8,9} the discrepancies becoming very important for nucleon energies below 300 MeV.

In the context of an interacting Fermi-gas model,^{14,16} the inclusive cross section per unit of normalization volume V becomes

$$\frac{1}{V} \left[\frac{d^2\sigma}{d\Omega d\omega} \right]_{\text{NM}} = n_{\text{eff}}(k_F) X_{\text{NM}}(q, \omega; k_F), \quad (8)$$

where $n_{\text{eff}}(k_F)$ is the effective density of target particles,^{3,4} X_{NM} is the nuclear matter inclusive cross section per particle,

$$X_{\text{NM}}(q, \omega; k_F) = K(k'/k) \int d\mathbf{p} \langle \frac{1}{2}(\mathbf{k}' - \mathbf{p} - \mathbf{q}) | t(E/2) | \frac{1}{2}(\mathbf{k} - \mathbf{p}) \rangle_A |^2 S_{\text{NM}}(\mathbf{p}, \mathbf{p} + \mathbf{q}; \omega), \quad (9)$$

and $\mathbf{q} = \mathbf{k} - \mathbf{k}'$ is the momentum transfer to the target. The nuclear matter structure function S_{NM} is given by

$$S_{\text{NM}}(\mathbf{p}, \mathbf{p} + \mathbf{q}; \omega) = \frac{3}{16\pi k_F^3} \int dz A_h(\mathbf{p}; z) A_p(\mathbf{p} + \mathbf{q}; z + \omega) \theta(\epsilon_F - z) \theta(z + \omega - \epsilon_F), \quad (10)$$

where $A_{h,p}$ is the hole (particle) spectral function.¹² It is this structure function and $n_{\text{eff}}(k_F)$ which depend on the details of the particular model of nuclear matter used. In the present Fermi-gas model, we assume a quasiparticle approximation^{15,17} for the hole states ($z < \epsilon_F$), namely,

$$A_h(\mathbf{p}; z) \simeq \rho(p) \delta(z - e(p)), \quad (11)$$

with $e(p)$, the energy of the hole in the nuclear medium, determined from

$$e(p) - \frac{p^2}{2m} - \text{Re}[U_{\text{NM}}(p; e(p))] = 0. \quad (12)$$

U_{NM} is the complex self-energy determined from a self-consistent calculation in nuclear matter with characteristic Fermi momentum k_F . The probability $\rho(p)$ is defined, in the quasiparticle approximation,¹⁵ by

$$\rho(p) = \left[\left| 1 - \frac{\partial}{\partial z} \{ \text{Re}[U_{\text{NM}}(p; z)] \} \right|_{z=e(p)} \right]^{-1}. \quad (13)$$

In practice, we shall take $\rho(p) \simeq 1$. The particle states are described "exactly" in the nuclear matter model:

$$A_p(p; z) = -\frac{1}{\pi} \frac{\text{Im}[U_{\text{NM}}(p; z)]}{[E_{\text{NM}}(p; z)]^2 + \{\text{Im}[U_{\text{NM}}(p; z)]\}^2}, \quad (14)$$

with

$$E_{\text{NM}}(p; z) = z - \frac{p^2}{2m} - \text{Re}[U_{\text{NM}}(p; z)]. \quad (15)$$

With the above approximations for the hole and particle spectral functions, the structure function becomes [using Eqs. (10)–(15)]

$$S(\mathbf{p}, \mathbf{p} + \mathbf{q}; \omega) = \frac{3}{16\pi^2 k_F^3} \frac{\text{Im}[U_{\text{NM}}(\mathbf{p} + \mathbf{q}; e(p) + \omega)]}{[E(\mathbf{p} + \mathbf{q}; e(p) + \omega)]^2 + \{\text{Im}[U_{\text{NM}}(\mathbf{p} + \mathbf{q}; e(p) + \omega)]\}^2} \theta[\epsilon_F - e(p)] \theta[e(p) + \omega - \epsilon_F]. \quad (16)$$

This approach accounts for 2p-2h propagation in the polarization propagator.¹⁰ In our model, the width of the particle states is given by the imaginary part of the self-energy calculated self-consistently in the interacting medium. The imaginary part of U_{NM} was taken from the parametrization given in Table 4 of Ref. 14. Equation (14) requires the self-energy off shell, a quantity rarely calculated in the nuclear medium. Therefore, we have approximated z in Eq. (14) by its on-shell value prescribed by the quasiparticle approximation [Eq. (12)]; i.e., $e(p) + \omega \simeq e(\mathbf{p} + \mathbf{q})$ in E and in $\text{Im}(U_{\text{NM}})$ in Eq. (16).

Equation (9) shows the interplay between the momentum-dependent and generally off-shell NN amplitude and the structure function. The fact that the an-

tisymmetrized matrix elements of the force depend not only on the transferred momentum \mathbf{q} , but also on the momenta of the struck and outgoing nucleons precludes an exact factorization of the cross section in terms of the nucleon-nucleon cross section and the usual nuclear response function. This is easily seen by considering an effective force which is local in coordinate space. In this case we have the following formal dependence on the momentum coordinates:

$$\langle \frac{1}{2}(\mathbf{k}' - \mathbf{p} - \mathbf{q}) | t(E/2) | \frac{1}{2}(\mathbf{k} - \mathbf{p}) \rangle_A = t(\mathbf{q}; E/2) - t(\mathbf{p} - \mathbf{k}'; E/2), \quad (17)$$

indicating that the exchange (second) term of the in-

interacting pair couples the momentum-dependent nucleon-nucleon t matrix to the S_{NM} function. If the momentum of the struck particle \mathbf{p} is neglected or approximated by a "fixed" value in Eq. (17), the inclusive cross section takes the standard factorized form in terms of the nucleon-nucleon cross section in the medium and the nuclear response. We shall return to this point later in this section.

The problem of accounting for the finite size of the target can be addressed in the context of a local-density approximation. Indeed, the inclusive cross section calculated in Eq. (8) is characterized by the Fermi momentum of the system. Allowing k_F to follow the nuclear density of the target,

$$\rho(r) = \frac{2}{3\pi^2} k_F^3(r), \quad (18)$$

we can write the inclusive cross section for a finite target as

$$\frac{d^2\sigma}{d\Omega d\omega} = \int d\mathbf{r} n_{\text{eff}}(r) X_{\text{NM}}(q, \omega; k_F(r)), \quad (19)$$

with

$$n_{\text{eff}}(r) = \rho(r) A(r). \quad (20)$$

$\rho(r)$ is the nuclear density obtained in the present work from a single-particle model description of electron scattering and single-particle energies.⁸ $A(r)$ is the attenuation of the incident and outgoing flux in the medium calculated in an eikonal approximation.^{3,4} In particular,

$$A(r) = \frac{1}{2} \int d(\cos\theta) \left[\exp \left[-2 \int_{-\infty}^r \eta_{\text{in}}(z) dz \right] \right. \\ \left. \times \left[\exp \left[-2 \int_r^{\infty} \eta_{\text{out}}(z') dz' \right] \right] \right], \quad (21)$$

where

$$\eta_j = \frac{m}{(\hbar c)^2 k_j} \text{Im}[U_{\text{NM}}(k_F, E_j)]. \quad (22)$$

m is the nucleon mass, k_j is the local initial (in) or final (out) momentum, and E_j is the initial or final asymptotic kinetic energy of the projectile. The vector \mathbf{r} locates the position of the inelastic collision and is given in terms of

$$X_{\text{NM}}^{\text{opt}}(q, \omega; k_F) = K(k'/k) \left| \langle \frac{1}{2}(\mathbf{k}' - \mathbf{p}_{\text{opt}} - \mathbf{q}) | t(E/2) | \frac{1}{2}(\mathbf{k} - \mathbf{p}_{\text{opt}}) \rangle_A \right|^2 R_{\text{NM}}(q; \omega), \quad (26)$$

and R_{NM} the nuclear matter response function,

$$R_{\text{NM}}(q; \omega) = \int d\mathbf{p} S_{\text{NM}}(\mathbf{p}, \mathbf{p} + \mathbf{q}; \omega). \quad (27)$$

Equation (25) is the factorized inclusive cross section in terms of the nuclear response function. Although Eq. (26) is attractive in the sense that experiment would provide a direct measurement of $R(q, \omega)$, its validity depends on the momentum dependence of the effective force, the incident energy, and the excitation energy of the target. The approximate inclusive cross section is generalized to

(r, θ, φ) with the z axis taken along \mathbf{k}_{in} . The primed quantities in the second exponential remind us that the integration there is along the direction of the scattered nucleon. The local-density approximation in which $k_F = k_F(r)$ allows us to average contributions to the inclusive cross section throughout the target and obtain a parameter-free model.

Different approximations may be developed to simplify the structure of the inclusive cross section; their validity will depend on the energy range considered and on how relevant are the contributions from nucleons inside the nucleus. In the context of a local (apart from exchange terms) force as is considered here, one alternative is to neglect the \mathbf{p} dependence of the exchange term in the internucleon force, valid when the momentum of the outgoing particle has a magnitude $|\mathbf{k}'| \gg |\mathbf{p}|$. This approximation should be most reliable at relatively high incident energies ($\gtrsim 300$ MeV) and when the energy loss is much smaller than the incident energy ($\omega \ll E$). Another alternative is to choose an "optimal" value for \mathbf{p} ,^{4,18} such that the effective force stays, at least, half on shell in the sense that the relative momenta before and after the collision are equal. This is ensured by taking

$$\mathbf{p} \rightarrow \mathbf{p}_{\text{opt}} = \alpha \mathbf{q}, \quad (23)$$

with

$$\alpha = -\frac{1}{2} \left[1 - \frac{k^2 - k'^2}{q^2} \right]. \quad (24)$$

We have adopted this optimal scheme to simplify the inclusive cross section while keeping the energy of the effective force fixed at $E/2$. This scheme differs from that used by Smith and Bozoian^{4,6} and is similar to the procedure used in Ref. 18. In particular, the present scheme retains may of the off-shell effects of the force present in the more complete expression [Eq. (9)].

In the context of the optimal approximation, we obtain, for the inclusive cross section per unit of volume in nuclear matter,

$$\frac{1}{V} \left[\frac{d^2\sigma}{d\Omega d\omega} \right]_{\text{NM}}^{\text{opt}} = n_{\text{eff}}(r) X_{\text{NM}}^{\text{opt}}(q; \omega; k_F), \quad (25)$$

where

include finite-size effects in exactly the same way as that which led to Eq. (19).

III. RESULTS

We have performed calculations of exact [Eq. (19)] and factorized [Eq. (25)] inclusive cross sections in order to test the validity of the latter. The nuclear matter results required for the calculation of the structure and response functions were taken from Refs. 14 and 16. We have used the energy-dependent t -matrix interaction of Ref. 19

based on the SP84 phase shifts of Arndt *et al.*²⁰ for the projectile-nucleon coupling with its central, spin-orbit, and tensor components evaluated at the energies studied. Although this effective force does not include explicit medium corrections, we have verified that analogous calculations using the Paris-Hamburg density-dependent force²¹ lead to similar conclusions regarding the relative differences between the exact and approximate approaches for calculating the scattering observables. The distortion in the initial and final channels was estimated following the work by Smith and Bozoian⁶ including an explicit evaluation of $A(r)$ in Eq. (21).

In order to compare the two approaches for evaluating the exchange terms, we have chosen to calculate inclusive proton scattering from ^{40}Ca at 100 and 300 MeV. We examine the unpolarized inclusive cross section $d^2\sigma/d\Omega d\omega$, the spin-flip probability normal to the scattering plane S_{nn} , and the analyzing power A_y as typical observables of experimental interest in the inclusive process. In particular, we consider the ratios between the optimal and exact results:

$$R(\sigma) = \frac{(d^2\sigma/d\Omega d\omega)^{\text{opt}}}{(d^2\sigma/d\Omega d\omega)^{\text{exact}}}, \quad (28)$$

$$R(A_y) = \frac{(A_y)^{\text{opt}}}{(A_y)^{\text{exact}}}, \quad (29)$$

and

$$R(S_{nn}) = \frac{(S_{nn})^{\text{opt}}}{(S_{nn})^{\text{exact}}}. \quad (30)$$

Each observable was calculated using standard formulas²² for the partially inclusive cross sections $\sigma(m_i \rightarrow m_f)$ in which the spin projections of the projectile (m_i) and ejectile (m_f) normal to the scattering plane are regarded as known.

Figure 1 shows a plot of the ratios between the optimal and exact results as a function of (ω/E) and for asymptotic momentum transfer $q_{\text{asym}} = 0.5$ (dotted curve), 1.0 (dot-dashed curve), 1.5 (short-dashed curve), 2.0 (long-dashed curve), and 2.5 fm^{-1} (solid curve) at an incident laboratory energy for the proton of $E = 100$ MeV. For the ratio of the cross sections, we observe differences ranging from 10% to 20% depending on the momentum transfer, with the approximate results rapidly deteriorating as the maximum energy loss which can kinematically support a given q transfer is approached. Similar effects are found for the ratio of the spin-flip probabilities where the optimal approach underestimates S_{nn} at low q transfer. At higher q and as a function of the excitation energy, the situation is reversed. The results indicate that the optimal approximation may give the incorrect magnitude and shape of the spin-flip probabilities as a function of the excitation energy. The differences are even larger for the ratio of the analyzing powers and suggest that the factorized calculations are unreliable for A_y at this energy. The main reasons for the discrepancies between the calculated spin observables are the relatively poor treatments of the spin-orbit and tensor components of the effective interaction in the optimal scheme. By

fixing the magnitude and direction of the momentum of the struck nucleon in the target as implied by Eqs. (23) and (26), the effective force fails to sample correctly the structure function of Eq. (9).

As the energy of the incident proton increases, the exact and approximate calculations of the cross section and spin observables tend to agree better. In Fig. 2 we show the ratios between the optimal and exact results in the case of 300-MeV proton inelastic scattering from ^{40}Ca . Overall, the results agree to within 10% for the observables considered, except near the region of maximum energy loss allowed for a given momentum transfer q . Whenever the condition $(k^2 - k'^2) \geq q^2$ in the optimal choice for the struck nucleon, then $\alpha \geq 0$ in Eq. (24), and \mathbf{p}_{opt} , pointing in the direction of the momentum transfer \mathbf{q} , may reach a magnitude too large to be physically

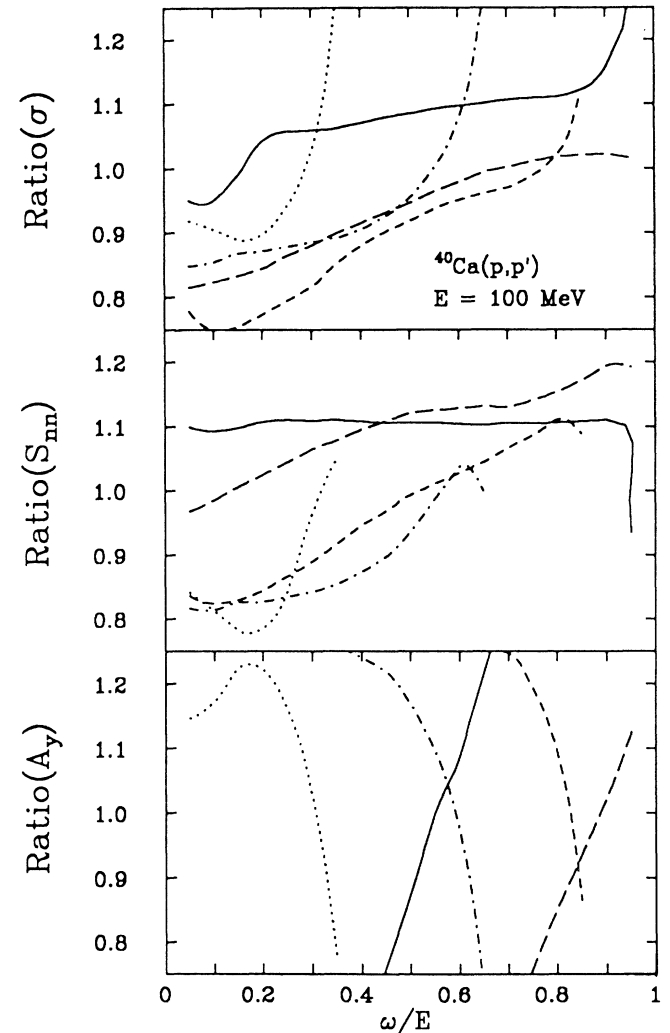


FIG. 1. Ratios between the approximate and exact results for the inclusive cross sections, spin-flip probabilities, and analyzing powers for proton inclusive scattering from ^{40}Ca at 100 MeV at different asymptotic momentum transfers. Dotted curves correspond to $q_{\text{asym}} = 0.5 \text{ fm}^{-1}$, dot-dashed curves to $q_{\text{asym}} = 1.0 \text{ fm}^{-1}$, short-dashed curves to $q_{\text{asym}} = 1.5 \text{ fm}^{-1}$, long-dashed curves to $q_{\text{asym}} = 2.0 \text{ fm}^{-1}$, and solid curves to $q_{\text{asym}} = 2.5 \text{ fm}^{-1}$. The effective NN interaction was taken from Ref. 19.

representative of the target particle momenta. Furthermore, the exchange contribution in the internucleon force will be evaluated at an unreasonable exchange momentum, yielding an inappropriate weighting of the direct and exchange parts. In particular, the exchange term associated with the central part of the force will be evaluated at small *exchange* momentum transfers where it is large. The resulting dominance of the central force in the approximate results near the region of maximum energy loss largely accounts for the overestimate of the cross-section ratio and underestimate of the A_y ratio in this kinematic region. At 300 MeV, the spin-flip probability shows greater disagreement than A_y or σ , with the approximate calculations systematically underestimating the exact ones.

The results shown in Figs. 1 and 2 at constant asymptotic momentum transfer indicate already the sensitivity of the inclusive observables to coupling effects. However, these conditions are unlikely to be met experimentally unless the measurements are made under special kinematic conditions. In order to analyze the implications of Figs. 1 and 2 under more realistic conditions, we have

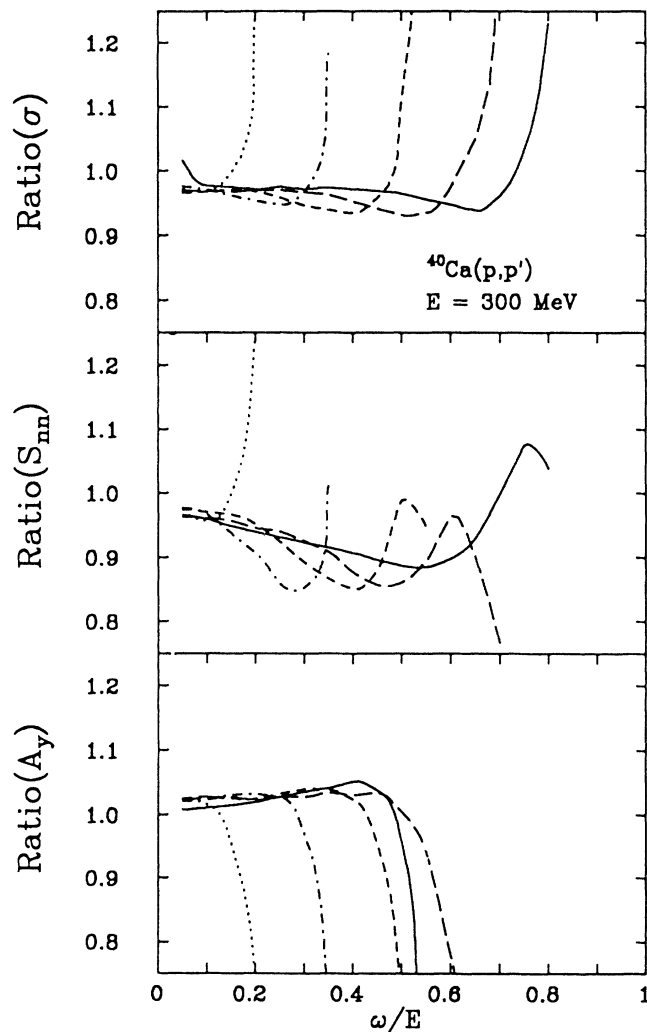


FIG. 2. Results for 300-MeV protons on ^{40}Ca for constant momentum transfers. See caption to Fig. 1.

calculated the cross section and spin observables S_{nn} and A_y at 100 and 300 MeV, choosing the laboratory scattering angle so as to have approximately the same range of momentum transfer as a function of the energy loss for the two energies. In Figs. 3–6 we show the observables for the exact (solid curves) and approximate (dot-dashed curves) calculations in proton inclusive scattering from ^{40}Ca corresponding to momentum transfers of roughly 0.5–1.5, 1.1–1.6, 1.5–2.0, and 2.2–2.5 fm^{-1} , respectively, as a function of the energy loss ω to the target. The momentum transfer as a function of ω is also illustrated. For 100-MeV protons we observe in Fig. 3 that the total cross section varies by about 5% over the small ω region, the difference between the exact and approximate calculations increasing to about 15% in the large ω region where $q \approx 0.5\text{--}1.5 \text{ fm}^{-1}$. The result is confirmed at $\theta = 30^\circ$ (Fig. 4) where the discrepancies are of the order of 15% for q between 1.1 and 1.6 fm^{-1} . For $\theta = 45^\circ$ (Fig. 5) the differences are again of the order of 10% where the cross section is large with the two approaches agreeing for $\omega > 75 \text{ MeV}$. For $q \approx 2.0\text{--}2.5 \text{ fm}^{-1}$ (Fig. 6) the cross sections differ by about 5%. We conclude that at 100 MeV the inclusive cross section does not show a large sensitivity to the presence of nonlocal couplings arising

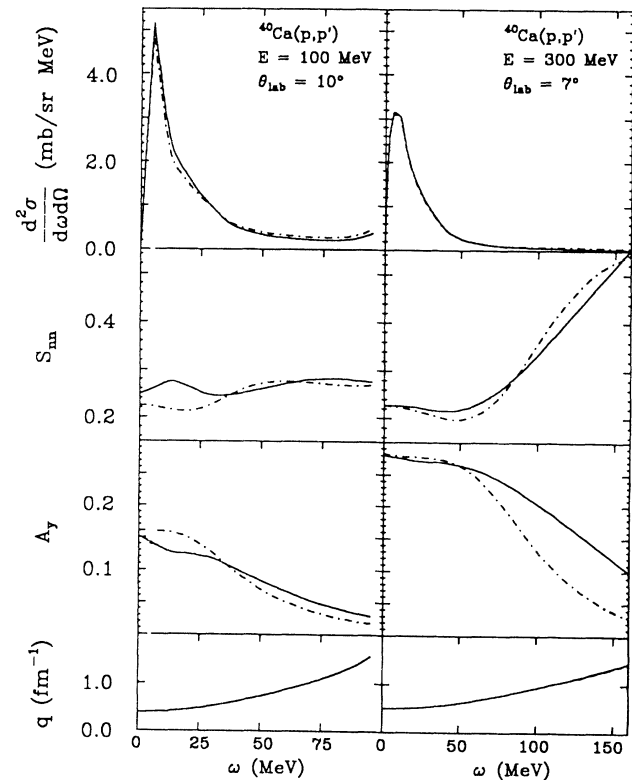


FIG. 3. Inclusive cross sections, spin-flip probabilities, and analyzing powers for inelastic proton scattering from ^{40}Ca at 100 MeV, 10° laboratory scattering angle, and 300 MeV, 7° laboratory scattering angle, respectively. Solid curves denote results from the exact calculation, while the dot-dashed curves denote results from the optimal approximation. The effective nucleon-nucleon interaction was taken from Ref. 19.

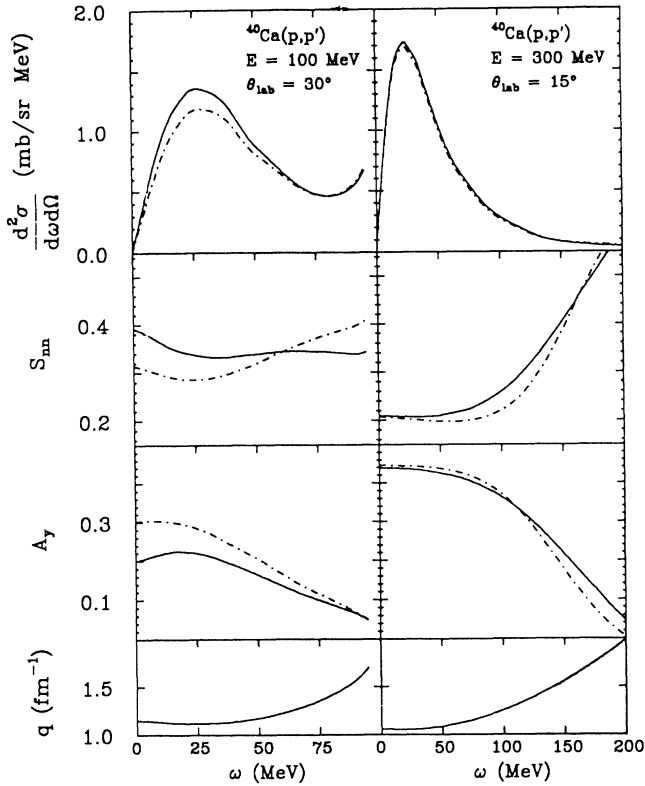


FIG. 4. Observables for 100- and 300-MeV protons at 30° and 15° laboratory scattering angle, respectively. See caption to Fig. 3.

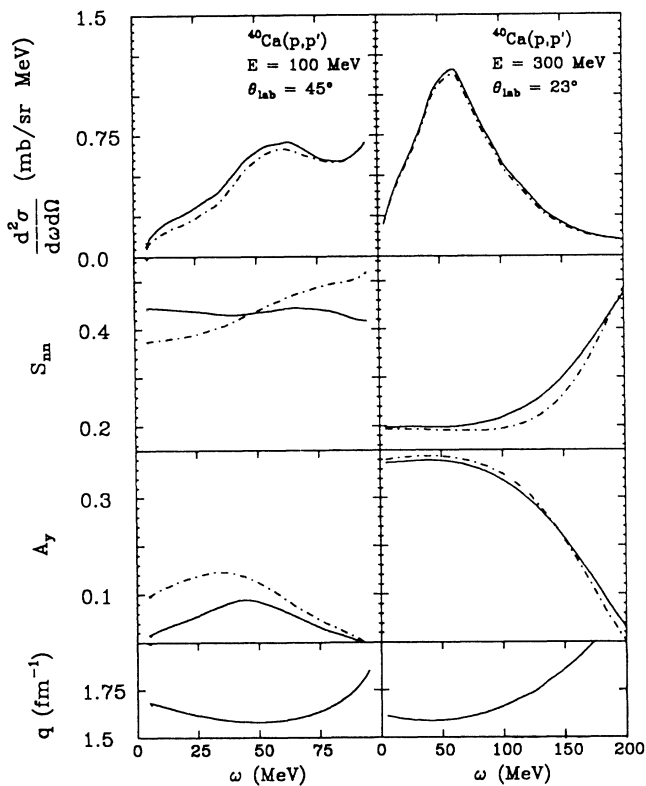


FIG. 5. Observables for 100- and 300-MeV protons at 45° and 23° laboratory scattering angle, respectively. See caption to Fig. 3.

from the exact treatment of exchange effects. Results using the factorized model remain in the region of 10–15 % discrepancy and exhibit the same general trends as the exact calculations. At 300 MeV, the inclusive cross sections differ by only about 5% over the q and ω range studied; the close agreement between the calculated cross sections at this energy is remarkable as shown in Figs. 3–6.

As concluded from Figs. 1 and 2, the spin observables show a greater sensitivity to the nonlocal exchange term in the effective interaction. For the 100-MeV results in Figs. 3–6, we observe large discrepancies in both the spin-flip probability and analyzing power results, suggesting that at energies near and below ~ 100 MeV the interpretation of the inclusive process in terms of a simple factorization of the cross sections can be misleading. The inclusive process samples aspects of nuclear structure beyond the usual response function. Correspondingly, nonlocal or velocity-dependent couplings between the projectile and struck nucleon are important. We have confirmed this point by performing similar calculations for 50-MeV protons on ^{40}Ca where the disagreement becomes important even for the cross sections. This point may be relevant for estimating single-particle contributions to the inclusive cross section in the preequilibrium region.⁶

At 300 MeV, the results for the cross section and the spin observables are in reasonably good agreement. As can be observed from Figs. 3–6, the major discrepancies

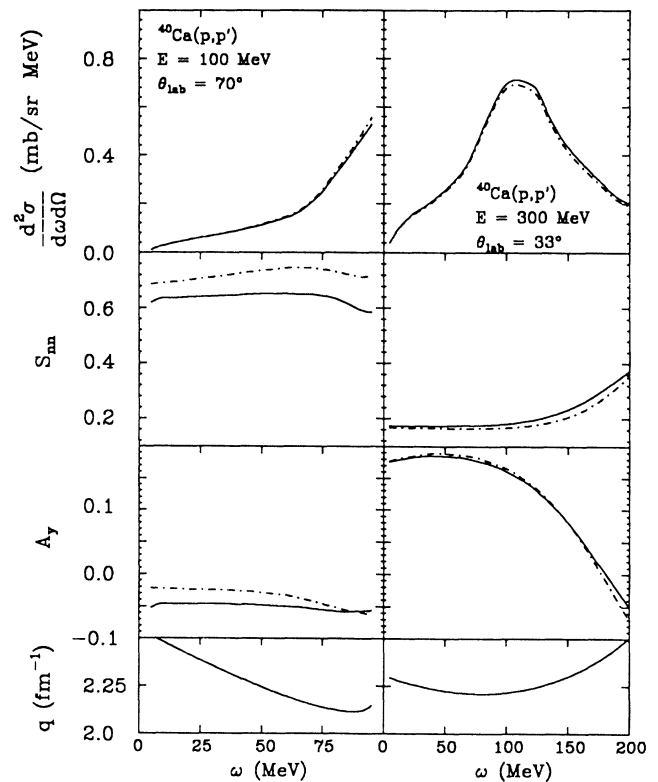


FIG. 6. Observables for 100- and 300-MeV protons at 70° and 33° laboratory scattering angle, respectively. See caption to Fig. 3.

remain in the spin observables especially for S_{nn} in the q region between 0.5 and 2.0 fm^{-1} and for A_y in the low- q region for excitation energies greater than 50 MeV. We have also investigated the convergence of the results at 500 MeV. The agreement between the exact and approximate calculations remains at the level of the results suggested by Figs. 3–6 at 300 MeV, the main differences still being primarily significant for the spin observables.

It may be argued that different approximations for the exchange term in the calculation of the observables might yield closer agreement to the exact results. We have checked this point by taking alternative prescriptions for the value of the momentum of the target nucleon, namely, $\mathbf{p}=0$, which neglects the role of the nucleon motion in the process, and $\mathbf{p}=-\mathbf{q}$, which has been used in the calculation of low- q and ω excitations in inelastic nucleon scattering to discrete states.²³ The first approximation ($\mathbf{p}=0$) works relatively better than the optimal choice at 500 MeV, but deteriorates rapidly as the energy of the incident particle decreases. The second approximation ($\mathbf{p}=-\mathbf{q}$) only works reasonably well in a very narrow range of q and ω and deteriorates quickly in the region of most interest in the inclusive processes.

Our primary emphasis in this work is on differences between exact and factorized inclusive results, and what these differences imply about the nuclear structure being sampled. We have, however, also examined differences in the calculated inclusive observables arising from the use of two different nucleon-nucleon interactions, namely, the free t -matrix interaction¹⁹ considered above and the Paris-Hamburg density-dependent force.²¹ As noted above, use of the density-dependent force leads to similar conclusions regarding the differences between exact and approximate approaches. In this comparison we will only consider results calculated exactly, i.e., using Eq. (19). This is relatively straightforward as each elementary cross section $X(q, \omega; k_F)$ is, like the density-dependent force, calculated at fixed values of k_F . Although it would be preferable to use a fully off-shell interaction as in Ref. 8, this is prohibitive at present.

Figures 7–10 show comparisons between the calculated inclusive observables using the free t -matrix interaction¹⁹ (dot-dashed curves) and the density-dependent force²¹ (solid curves) at 100 and 300 MeV incident proton energies (E) and over the same range of momentum transfer (q) and energy loss (ω) considered in Figs. 3–6. At 100 MeV, the largest difference between the two forces occurs in the calculated spin-flip probabilities normal to the scattering plane S_{nn} . For each force S_{nn} is predicted to vary rather slowly with ω . For the density-dependent force, S_{nn} also varies slowly with q , being near 0.4 over most of the (q, ω) considered. In contrast, the free t -matrix results for S_{nn} (at 100 MeV) are seen to change from ~ 0.25 for $q \lesssim 1 \text{ fm}^{-1}$ to ~ 0.6 for $q \gtrsim 2.0 \text{ fm}^{-1}$. This presumably reflects the dominance of both isoscalar and isovector longitudinal spin couplings ($\sigma \cdot \mathbf{q}$) known¹⁹ to be present in the free t -matrix interaction. The spin-dependent part of this same force is dominated by its transverse spin ($\sigma \times \mathbf{q}$) component at smaller momentum transfers, in qualitative agreement with the decrease in S_{nn} at smaller q (see Refs. 19 and 24).

At 100 MeV, the cross sections calculated using the two forces agree closely over the full (q, ω) range studied, even though each of them varies considerably with q and ω . The calculated A_y using the two forces at 100 MeV are seen to agree reasonably well.

In contrast to the results at 100 MeV, calculations at 300 MeV using the two forces differ considerably for each of the observables considered, especially A_y and the differential cross sections. In particular, the differential cross section calculated with the density-dependent force is larger than that calculated using the free t matrix for all q and ω . The ratio of the peak cross sections varies from ~ 1.3 near $q=0.5 \text{ fm}^{-1}$ to ~ 2.0 near $q=2.2 \text{ fm}^{-1}$. The A_y calculated using the density-dependent force is larger (smaller) than that obtained with the free t matrix near the peak at small (large) momentum transfer. The trend of the calculated S_{nn} at 300 MeV is similar to that at 100 MeV, but less pronounced; the S_{nn} calculated using the free t matrix never becomes significantly larger than that obtained with the density-dependent force. The generally smaller values of S_{nn} calculated with the free t matrix at 300 relative to 100 MeV are consistent with the properties of the force shown in Ref. 19 where the longitudinal spin coupling at large q is much less dominant than at 100 MeV.

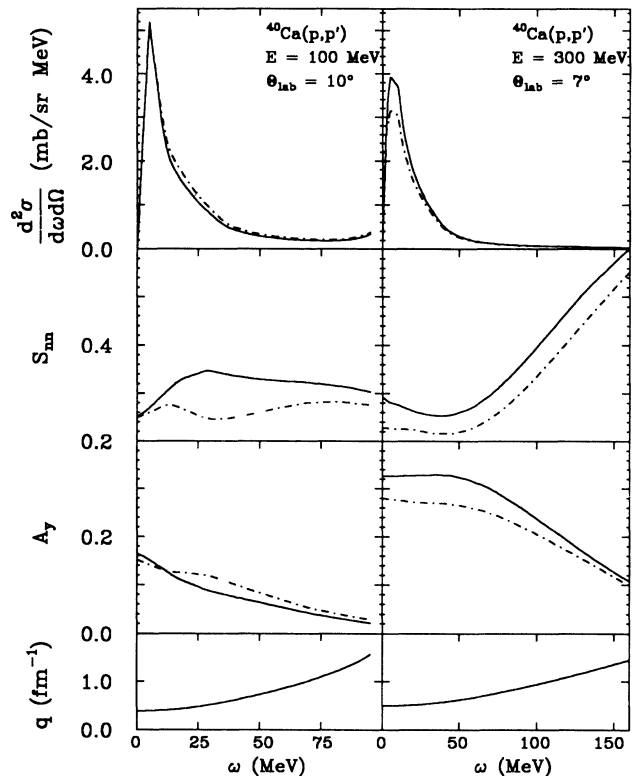


FIG. 7. Inclusive cross sections, spin-flip probabilities, and analyzing powers for inelastic proton scattering from ^{40}Ca at 100 and 300 MeV for laboratory scattering angles of 10° and 7° , respectively. The solid and dot-dashed curves correspond to the Paris-Hamburg density-dependent interaction and the free t -matrix interaction, respectively.

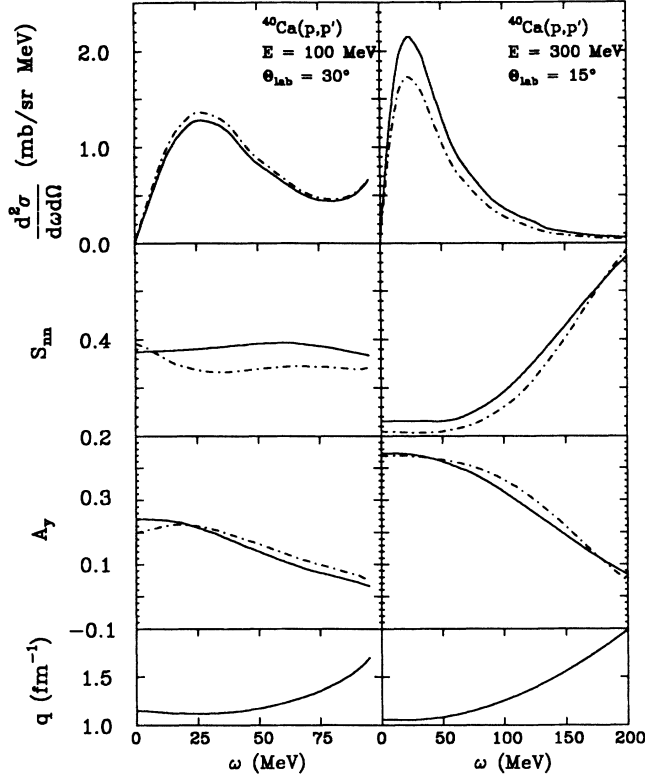


FIG. 8. Same as Fig. 7 at laboratory scattering angle of 30° and 15°.

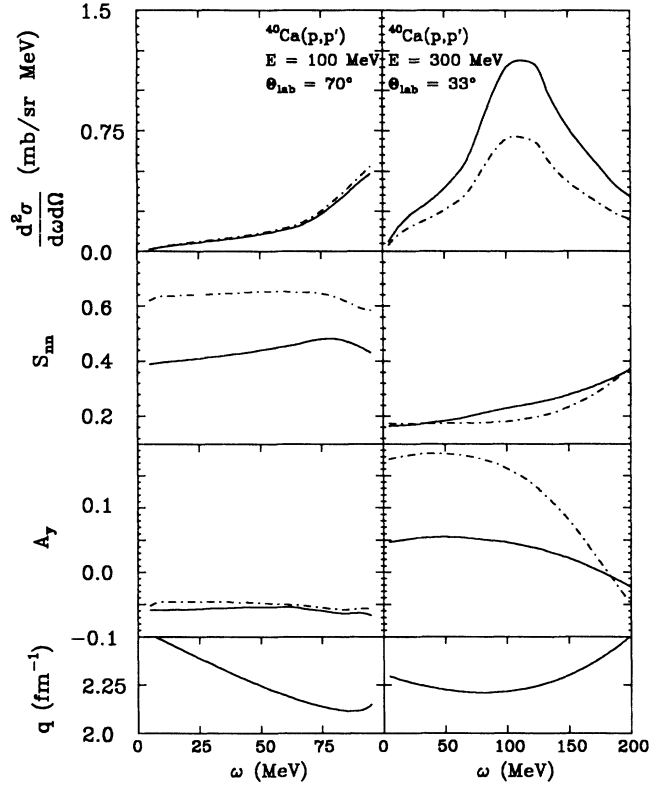


FIG. 10. Same as Fig. 7 at laboratory scattering angle of 70° and 33°.

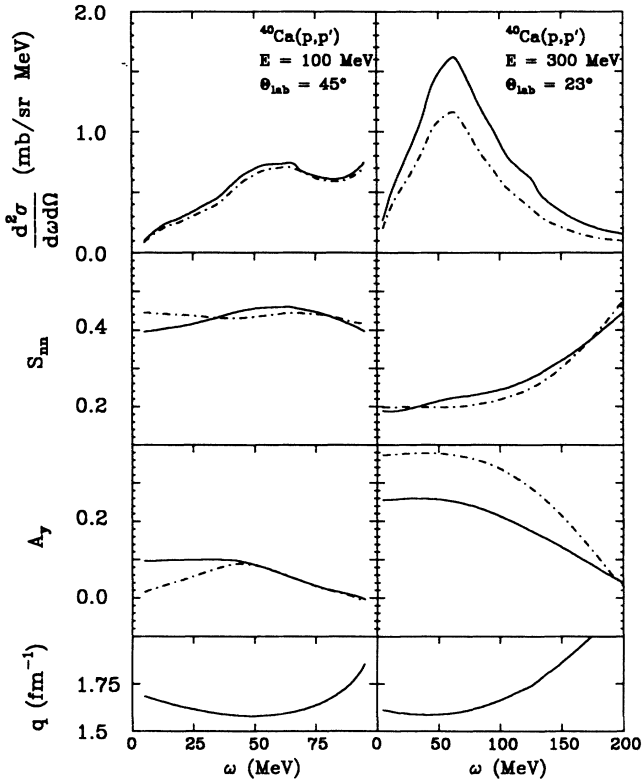


FIG. 9. Same as Fig. 7 at laboratory scattering angles of 45° and 23°.

IV. CONCLUSIONS

There exists a growing interest in understanding the different modes of nucleon-induced excitations over an increasingly wider range of momentum transferred to the target. In particular, the kinematical regime involving momentum transfers $q \approx 1.0\text{--}3.0 \text{ fm}^{-1}$ and energy losses $\omega = 0\text{--}200 \text{ MeV}$ is receiving considerable attention. This has led us to investigate the validity of the ansatz under which the experimental results can be interpreted in terms of the standard nuclear response function. We have considered an interacting Fermi-gas model to describe both the reaction and structure aspects of the inclusive process to first order in the respective nucleon-nucleon effective couplings. An extension of the local-density approximation has allowed us to apply the nuclear matter results to finite nuclei. Thus we have obtained a parameter-free model which should account, on the average, for the response of the entire nucleus. We have paid particular attention to those aspects which make nucleon inclusive scattering a different probing tool of the target response than other particles, namely, the indistinguishability of the projectile from the nucleons in the target and, more precisely, the associated nonlocal couplings. Furthermore, the model also provides a correct treatment of the off-shell characteristics of the in-nucleon effective interaction used, an aspect often neglected, but one which can be very important for describing the scattering of particles within the nuclear medium.

The present approach naturally leads to a result for the inclusive observables which indicates that, in principle, the nucleon-induced process samples the full nuclear structure function. In order to compare this model with the most widely used approaches, we have investigated different approximations which lead to factorized expressions for the observables in terms of the response function. Of the approximations considered, the one which best represents the exact calculations is a variant of the "optimal" factorization point of view. This choice implies selecting momenta for the struck particles in the target which ensure that the effective interaction is half on shell. The optimal prescription is also consistent with approximations developed for calculating intermediate-energy optical potentials where similar problems arise concerning the role of the effective internucleon force when simplifications are introduced.

We have performed calculations of the exact and approximate models, taking as a typical example proton inelastic scattering from ^{40}Ca at 100 and 300 MeV. Our results show that the spin observables are most sensitive to the correct antisymmetrization of the theory and to the associated off-shell properties of the nucleon-nucleon force. There is a clear indication that nucleon scattering probes information beyond the usual nuclear response function, and therefore models based on the simpler factorized assumption can lead to misinterpretations of scattering observables as a function of the excitation energy. Overall, the total inclusive cross section is the observable least sensitive to approximations to the exact calculation, especially in the region where the magnitudes of the cross sections are large enough to be relevant.

In quantitative terms, our calculations indicate that at proton energies of 300 MeV and above, the total inclusive cross sections calculated exactly are described in the approximate model with an accuracy on the order of 5%, systematically underestimating the exact results for $q > 1.5 \text{ fm}^{-1}$. The spin-flip probabilities are described to within 10–15% accuracy, being underestimated below and overestimated above $\omega \approx 80 \text{ MeV}$ for $q \approx 1.0 \text{ fm}^{-1}$ and systematically underestimated for the 200-MeV excitation energy range for $q > 1.0 \text{ fm}^{-1}$. The calculated analyzing powers differ at the 5–10% level, except in the regions of high excitation energy and small scattering angles. We conclude that above 300 MeV incident energy and within the q range $0.5\text{--}2.5 \text{ fm}^{-1}$ studied, measured observables should provide a reliable measure of the usual response function at the 10% level and that uncertainties of this order are intrinsic to the factorized model for describing or interpreting data.

As the energy of the incident nucleon decreases, the

agreement between the exact and approximate models deteriorates gradually. At 100 MeV incident energy, the two calculations disagree at the 15% level for the cross sections and at the 15–30% level for the spin observables. This suggests that at lower incident energies the nonlocal terms play a significant role, thus making the interpretation of observables solely in terms of the standard nuclear response function unreliable or at least suspect.

In addition to the primary objective of studying the implications of an approximate treatment of nonlocal couplings in the effective nucleon-nucleon force, we have also considered differences in the calculated inclusive observables arising from an "exact" treatment of two different internucleon interactions. In particular, we have compared results using the free t -matrix interaction of Ref. 19 and the density-dependent interaction of Ref. 21. Differences between results using these two nucleon-nucleon interactions should *not* be ascribed to medium modifications alone; these forces are known²⁴ to differ even at $k_F = 0$. Indeed, the largest differences in the calculated cross sections occur at 300 MeV where medium corrections of the type included are known to be relatively weak. Overall, the differences between results using the two interactions are comparable to, and often larger than, those found when comparing the exact factorized results for the same interaction.

Our conclusions regarding the reliability of factorized approximations to the calculation of inclusive observables are valid in the context of the model presented and its consistent reduction to a factorized form. The use of alternative prescriptions for the calculation of the nucleon-nucleon coupling in the medium could, of course, lead to either larger or smaller differences. The present results, together with similar ones obtained using the Paris-Hamburg force, are *representative* of those using presently available nucleon-nucleon effective forces. The use of more sophisticated forces which are intrinsically nonlocal and include a fully off-shell treatment of the nucleon-nucleon interaction is beyond the scope of this work.

ACKNOWLEDGMENTS

The authors thank H. Arellano for discussions and generous help. This work was supported in part by NSF Grant Nos. PHY-8607684 and PHY-8903856. We appreciate the generous amount of computer time provided by the Department of Physics and Astronomy and the University Computing and Networking Services Department of the University of Georgia. F.A.B. acknowledges partial support from FONDECYT Grant Nos. 1212-88 and 1239-90.

¹T. deForest and J. D. Walecka, *Adv. Phys.* **15**, 1 (1966).

²H. C. Chiang and J. Hufner, *Nucl. Phys.* **A349**, 466 (1980).

³G. F. Bertsch and O. Scholten, *Phys. Rev. C* **25**, 804 (1982); H. Esbensen and G. F. Bertsch, *Ann. Phys. (N.Y.)* **157**, 255 (1984).

⁴R. D. Smith, in *Proceedings of the International Conference on Spin Observables of Nuclear Probes, Telluride, Colorado, 1988*,

edited by C. J. Horowitz, C. D. Goodman, and G. E. Walker (Plenum, New York, 1988), p. 15.

⁵C. J. Horowitz and D. P. Murdock, *Phys. Rev. C* **37**, 2032 (1988).

⁶R. D. Smith and M. Bozoian, *Phys. Rev. C* **39**, 1751 (1989).

⁷W. G. Love, M. A. Franey, and F. Petrovich, of *Proceedings of the International Conference on Spin Excitations, Telluride*,

- Colorado, 1982*, edited by F. Petrovich *et al.* (Plenum, New York, 1984), p. 205.
- ⁸H. F. Arellano, F. A. Brieva, and W. G. Love, *Phys. Rev. C* **41**, 2188 (1990).
- ⁹Ch. Elster, Taksu Cheon, Edward Redish, and P. C. Tandy, *Phys. Rev. C* **41**, 814 (1990); R. Crespo, R. C. Johnson, and J. A. Tostevin, *ibid.* **41**, 2257 (1990).
- ¹⁰R. D. Smith and J. Wambach, *Phys. Rev. C* **38**, 100 (1988).
- ¹¹F. A. Brieva and M. A. Nagarajan, *Nucl. Phys.* **A452**, 221 (1986).
- ¹²A. L. Fetter and J. D. Walecka, *Quantum Theory of Many-Particle Systems* (McGraw-Hill, New York, 1971).
- ¹³M. Ichimura, K. Kawahigashi, T. S. Jorgensen, and C. Gaarde, *Phys. Rev. C* **39**, 1446 (1989).
- ¹⁴J. P. Jeukenne, A. Lejeune, and C. Mahaux, *Phys. Rev. C* **16**, 80 (1977).
- ¹⁵J. P. Jeukenne, A. Lejeune, and C. Mahaux, *Phys. Rep.* **25C**, 83 (1976).
- ¹⁶F. A. Brieva and J. R. Rook, *Nucl. Phys.* **A291**, 299 (1977).
- ¹⁷A. L. Fetter and K. M. Watson, *Advances in Theoretical Physics*, edited by K. A. Brueckner (Academic, New York, 1965), p. 115.
- ¹⁸A. Picklesimer, P. C. Tandy, R. M. Thaler, and D. H. Wolfe, *Phys. Rev. C* **30**, 1861 (1984).
- ¹⁹M. A. Franey and W. G. Love, *Phys. Rev. C* **31**, 488 (1985).
- ²⁰R. A. Arndt *et al.*, *Phys. Rev. D* **28**, 97 (1983); R. A. Arndt and L. D. Roper (unpublished).
- ²¹H. V. von Geramb and K. Nakano, in *Interaction Between Medium Energy Nucleons in Nuclei—1982*, Proceedings of the Workshop on the Interaction Between Medium Energy Nucleons in Nuclei, AIP Conf. Proc. No. 97, edited by H. O. Meyer (AIP, New York, 1983), p. 44.
- ²²R. Boyd, S. Davis, C. Glashauser, and C. F. Haynes, *Phys. Rev. Lett.* **23**, 1590 (1971).
- ²³F. Petrovich, H. McManus, V. A. Madsen, and J. Atkinson, *Phys. Rev. Lett.* **22**, 895 (1969); W. G. Love, *Nucl. Phys.* **A312**, 160 (1978); W. G. Love and M. A. Franey, *Phys. Rev. C* **24**, 1073 (1981); J. J. Kelley *et al.*, *ibid.* **39**, 1222 (1989).
- ²⁴W. G. Love, Amir Klein, M. A. Franey, and K. Nakayama, *Can. J. Phys.* **65**, 536 (1987).